

Controlled Cellular Delivery of Amphiphilic Cargo by Redox-Responsive Nanocontainers


Wilke C. de Vries, Sergej Kudruk, David Grill, Maximilian Niehues, Anna Livia Linard Matos, Maren Wissing, Armido Studer, Volker Gerke,* and Bart Jan Ravoo*

The specific transport of amphiphilic compounds such as fluorescently labeled phospholipids into cells is a prerequisite for the analysis of highly dynamic cellular processes involving these molecules, e.g., the intracellular distribution and metabolism of phospholipids. However, cellular delivery remains a challenge as it should not affect the physiological integrity and morphology of the cell membrane. To address this, polymer nanocontainers based on redox-responsive cyclodextrin (CD) amphiphiles are prepared, and their potential to deliver fluorescently labeled phospholipids to intracellular membrane compartments is analyzed. It is shown that mixtures of reductively degradable cyclodextrin amphiphiles and different phospholipids form liposome-like vesicles (CD–lipid vesicles, $C_{SS}LV$) with a homogeneous distribution of each lipid. Host–guest-mediated self-assembly of a cystamine-crosslinked polymer shell on these $C_{SS}LV$ produces polymer-shelled liposomal vesicles ($P_{SS}C_{SS}LV$) with the unique feature of a redox-sensitive $C_{SS}LV$ core and reductively degradable polymer shell. $P_{SS}C_{SS}LV$ show high stability and a redox-sensitive release of the amphiphilic cargo. Live cell experiments reveal that the novel $P_{SS}C_{SS}LV$ are readily internalized by primary human endothelial cells and that the reductive microenvironment of the cells' endosomes triggers the release of the amphiphilic cargo into the cytosol. Thus, $P_{SS}C_{SS}LV$ represent a highly efficient system to transport lipid-like amphiphilic cargo into the intracellular environment.

The transport of fluorescently labeled phospholipids into the cell's interior can permit a live cell analysis of dynamic membrane-related processes involving such lipids that include

Dr. W. C. de Vries, M. Niehues, M. Wissing, Prof. A. Studer, Prof. B. J. Ravoo
Center for Soft Nanoscience and Organic Chemistry Institute
Westfälische Wilhelms-Universität Münster
Busso-Peuss-Str. 10, Münster 48149, Germany
E-mail: b.j.ravoo@uni-muenster.de

S. Kudruk, Dr. D. Grill, A. L. L. Matos, Prof. V. Gerke
Institute of Medical Biochemistry
Center for Molecular Biology of Inflammation
Westfälische Wilhelms-Universität Münster
Von-Esmarch-Str. 56, Münster 48149, Germany
E-mail: gerke@uni-muenster.de

 The ORCID identification number(s) for the author(s) of this article can be found under <https://doi.org/10.1002/advs.201901935>.

© 2019 The Authors. Published by WILEY-VCH Verlag GmbH & Co. KGaA, Weinheim. This is an open access article under the terms of the Creative Commons Attribution License, which permits use, distribution and reproduction in any medium, provided the original work is properly cited.

DOI: 10.1002/advs.201901935

lipid transport, lipid microdomain formation, or the interaction of lipids with membrane proteins.^[1–16] An important prerequisite for such studies is a mode of intracellular delivery that does not impair the physiological integrity of the cell membrane. Fusogenic liposomes have been introduced to integrate amphiphilic lipids into the plasma membrane; however, the presence of fusogenic lipids in these systems can affect membrane properties.^[6] Other approaches used pH-responsive polymersomes as delivery vehicles.^[16] Such polymersomes, initially reported by Armes and co-workers, are based on diblock copolymers consisting of a hydrophilic poly(2-(diisopropylamino) ethyl methacrylate) (PDPA) block and a hydrophobic poly(2-(methacryloyloxy) ethyl phosphorylcholine) (PMPC) block.^[17] Hydrophilic cargo encapsulated in the polymersomes could be released by protonation of the PDPA blocks and a resulting disassembly most likely occurring in the acidic late-endosomal/lysosomal cell compartment. A different approach to generate responsive vehicles for amphiphile

delivery is based on amphiphilic cyclodextrin (CD) derivatives, in which the hydrophilic cyclodextrin headgroup is connected via a disulfide (ss) bridge to hydrophobic alkyl chains of different lengths, thereby introducing a reductively cleavable bond.^[18] Such cyclodextrin vesicles were shown to trap hydrophobic dyes that could be released by reductive degradation. Here, we employed similar CD vesicles as basis for novel redox-sensitive nanocontainers permitting the efficient transport of amphiphilic phospholipids into cells.

The rationale of our approach is outlined in **Figure 1**. Cargo lipids and reductively cleavable β -cyclodextrin amphiphiles (β - CD_{SS}) were co-assembled into liposome-like cyclodextrin vesicle templates and decorated by host–guest chemistry with a reductively cleavable polymer shell.

Reductively cleavable β - CD_{SS} were synthesized as described^[19] and mixed with different phospholipids to generate redox-sensitive mixed CD–lipid vesicles ($C_{SS}LV$). Different β - CD_{SS} /lipid mixtures were tested for miscibility and stability, and a ratio of 50 mol% of the reductively cleavable β - CD_{SS} , 25 mol% 1-palmitoyl-2-oleoyl-*sn*-glycero-3-phospho-(1'-rac-glycerol) (POPG), 20 mol% 1,2-dioleoyl-*sn*-glycero-3-phosphate (DOPA),

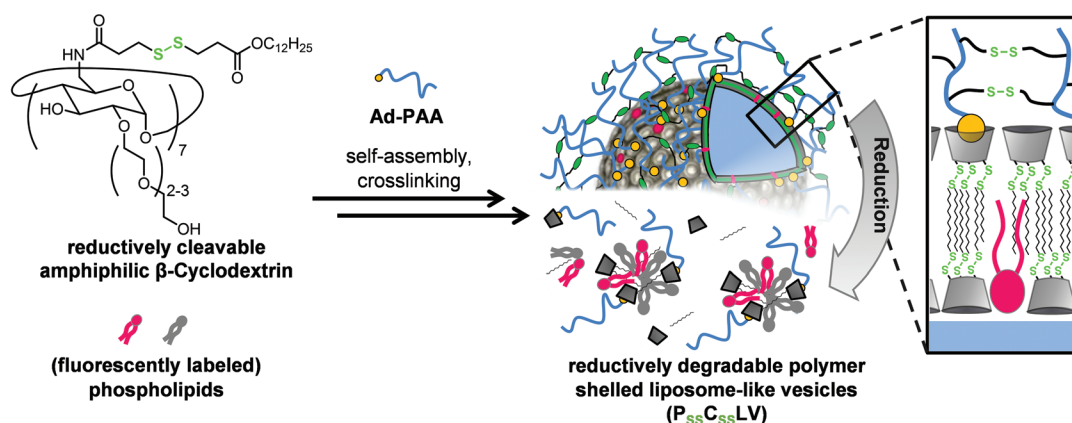


Figure 1. Schematic representation of the assembly and structure of $\text{P}_{\text{SS}}\text{C}_{\text{SS}}\text{LV}$, which entirely dissociate into smaller molecular units by cleavage of the disulfide bonds of both, the cyclodextrin core and the polymer shell.

and 5 mol% 1,2-dioleoyl-*sn*-glycero-3-phosphocholine (DOPC) was chosen for further experiments. Miscibility was verified by employing β -CD_{SS}/lipid giant unilamellar vesicles ($\text{C}_{\text{SS}}\text{L-GUV}$). Figures S1–S4 (Supporting Information) show that TopFluor (TF)- or nitrobenzoxadiazole (NBD)-labeled phospholipids (phosphatidylcholine (PC), phosphatidic acid (PA), phosphatidylinositol (PI), phosphatidylinositol-4,5-bisphosphat (PI(4,5)P₂)) assume a homogeneous distribution in the mixed β -CD_{SS}/lipid vesicles and that the β -CD_{SS}, which were labeled with adamantane-terminated rhodamine B (Ad-TEG-RhB) by host–guest recognition, are also homogeneously distributed.

The CD/lipid mixtures were then extruded to yield vesicles with an average hydrodynamic diameter of $d_h \approx 120$ nm and a ζ -potential of $\zeta \approx -8$ mV that remained stable over several days and also tolerated the incorporation of fluorescently labeled lipid derivatives. In a next step, the $\text{C}_{\text{SS}}\text{LV}$ were covered with a disulfide-crosslinked polymer shell by attaching adamantane-terminated polyacrylic acid (Ad–PAA) via host–guest interaction.^[19] The formation of homogeneous particles, herein referred to as polymer-shelled cyclodextrin lipid vesicles ($\text{P}_{\text{SS}}\text{C}_{\text{SS}}\text{LV}$), was assessed by dynamic light scattering (DLS), Fourier-transform infrared (FT-IR) spectroscopy, and ζ -potential measurements. This revealed an increase of the hydrodynamic radius by 25 nm and a decrease in the ζ -potential from $\zeta = -7.5$ mV to $\zeta = -19$ mV due to deprotonation of acrylic acid moieties of the polymer chain in $\text{P}_{\text{SS}}\text{C}_{\text{SS}}\text{LV}$. The stability of the polymer shell was then increased by 1-ethyl-3-(3-dimethylaminopropyl)carbodiimide (EDC)-mediated crosslinking yielding an amide bond with cystamine. During this step, no significant change of the hydrodynamic diameter but an increase of the ζ -potential to $\zeta = -12$ mV was observed due to the conversion of carboxylic acid to the amide. The successful conversion was also recorded via FT-IR spectroscopy revealing a decrease of the C=O stretching band of the carboxylic acid and a simultaneous increase of the amide absorption bands (Figure S5, Supporting Information).

$\text{P}_{\text{SS}}\text{C}_{\text{SS}}\text{LV}$ contain many disulfide bonds and should disintegrate in a reductive environment. This was analyzed by treatment with the thiol-based reducing agent dithiothreitol (DTT). Prior to addition of a reducing agent, $\text{P}_{\text{SS}}\text{C}_{\text{SS}}\text{LV}$ show an average hydrodynamic diameter of $d_h \approx 145$ nm and appear as

circular, flattened objects in transmission electron microscopy (TEM) images (Figure 2), typically observed for vesicles and polymer capsules.^[20–23] Incubation with DTT led to a change in morphology and a pronounced decrease in size (Figure 2). The reductive disintegration of $\text{P}_{\text{SS}}\text{C}_{\text{SS}}\text{LV}$ could be followed by recording the intensity of scattered light as a function of time revealing the colloidal stability of $\text{P}_{\text{SS}}\text{C}_{\text{SS}}\text{LV}$ in the absence of DTT and, upon addition of DTT, a pronounced decrease (Figure S6, Supporting Information).

We next assessed whether the reductive disintegration is accompanied by a release of the cargo lipids. Therefore, we performed Förster resonance energy transfer (FRET) experiments employing two populations of $\text{P}_{\text{SS}}\text{C}_{\text{SS}}\text{LV}$, one loaded with rhodamine B-labeled phosphatidylethanolamine (PE) and another with NBD-labeled PE. Although no significant decrease in the fluorescence of NBD ($\lambda_{\text{em}} = 527$ nm) was observed upon mixing with the rhodamine–PE labeled $\text{P}_{\text{SS}}\text{C}_{\text{SS}}\text{LV}$ in the absence of a reducing agent, addition of DTT led to a decrease in NBD fluorescence and a concomitant increase in the fluorescence of rhodamine B, suggesting FRET due to close proximity (distance < 10 nm) of the two fluorophore-labeled lipids (Figure S6 and kinetics in Figure S7, Supporting Information). Most likely, disintegration of $\text{P}_{\text{SS}}\text{C}_{\text{SS}}\text{LV}$ had resulted in a dynamic distribution and thus mixing of the cargo lipids within the smaller aggregates identified by DLS and TEM (Figure 2). To verify the specific redox sensitivity of the nanocontainers, we performed control experiments with polymer-shelled cyclodextrin liposomal vesicle (PCLV) devoid of reductively cleavable disulfide bonds. Therefore, the β -CD_{SS} were replaced by redox-stable cyclodextrin amphiphiles,^[24,25] and 2,2'-(ethylenedioxy)bis(ethylamine) was used for crosslinking of the polymer shell.^[26] These PCLV remained stable under reducing conditions, i.e., addition of DTT did not result in a change of size distributions or an altered FRET (Figure S6, Supporting Information) verifying that disintegration of $\text{P}_{\text{SS}}\text{C}_{\text{SS}}\text{LV}$ is caused by reduction of the disulfide bonds. In another set of controls, we assessed whether a cleavage of the polymer shell alone might already facilitate a release of cargo lipids. Therefore, $\text{P}_{\text{SS}}\text{CLV}$ containing only a reductively cleavable polymer shell but a redox-stable CD vesicle template were synthesized. Figure S6 (Supporting Information) shows that $\text{P}_{\text{SS}}\text{CLV}$ behave like PCLV, indicating that a release

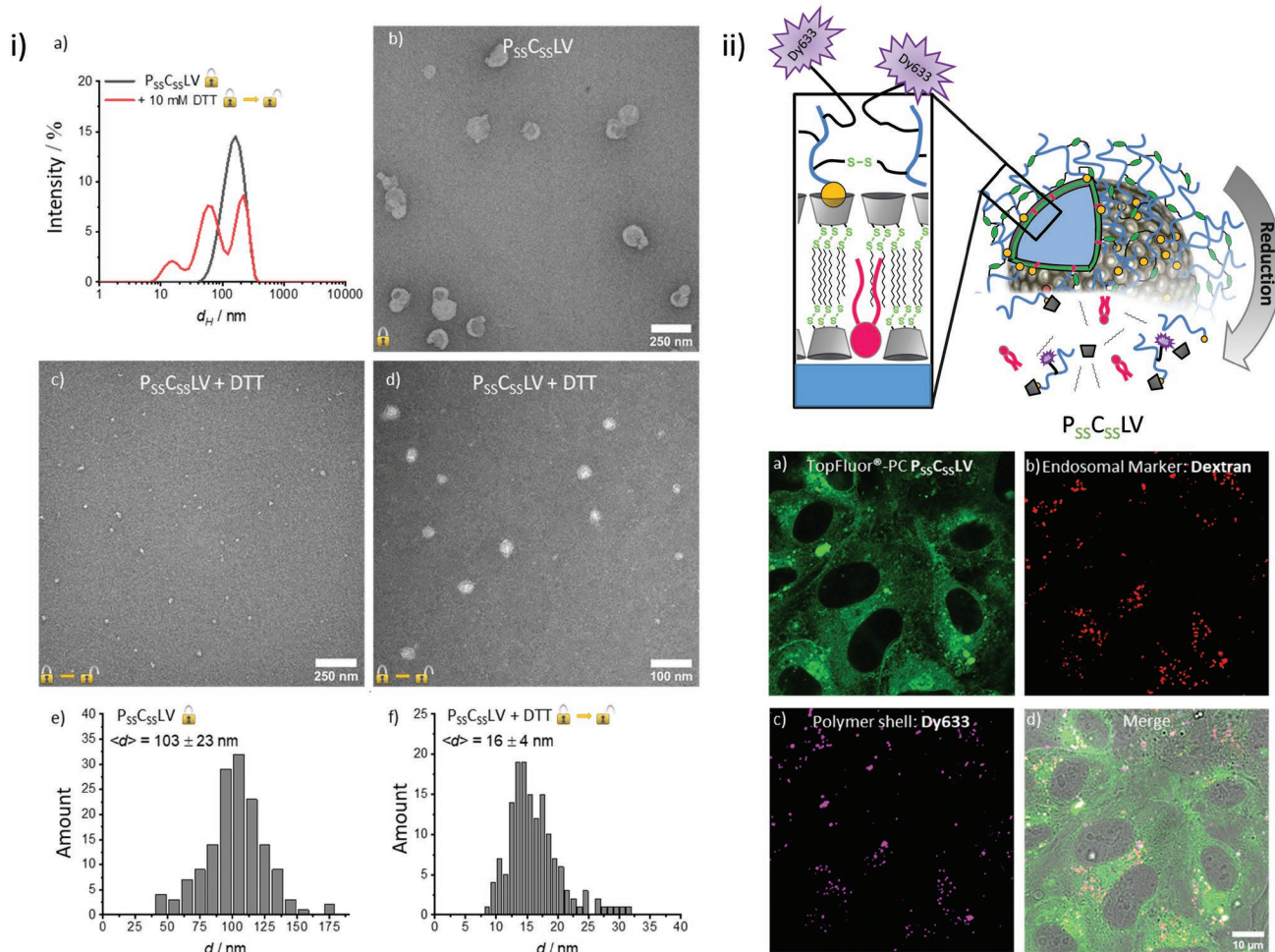


Figure 2. Morphology and cellular delivery of $P_{55}C_{55}LV$. i) Size change due to reductive disassembly of the nanocontainers. a) Intensity-weighted size-distribution of $P_{55}C_{55}LV$ determined by DLS before and after treatment with 10×10^{-3} M DTT. A CONTIN-algorithm for polydisperse samples was used for the analysis. b) TEM images of $P_{55}C_{55}LV$. c,d) TEM images following reductive cleavage. After 24 h of incubation in 10×10^{-3} M DTT, samples were negatively contrasted by 0.5% (w/v) tungstophosphoric acid. e,f) Size distribution of $P_{55}C_{55}LV$ determined by TEM e) before and f) after 24 h incubation in 10 mM DTT. ii) Intracellular delivery of TF-PC incorporated into $P_{55}C_{55}LV$. Top: Schematic representation of the structure of $P_{55}C_{55}LV$ containing a Dy633-labeled polymer shell. Bottom: HUVEC were incubated for 2 h with Dy633-labeled $P_{55}C_{55}LV$ containing TF-labeled PC and analyzed by confocal microscopy. Images show the uptake of the $P_{55}C_{55}LV$ and the intracellular release of TF-PC. The fluorescent label of the polymer shell, Dy633, is retained in endosomal structures as revealed by labeling with co-internalized RhB-dextran.

of cargo lipids requires both, a cleavable polymer shell and a reductively degradable vesicle template.

PC-derivatives represent the main lipid species in mammalian membranes^[27] and thus were chosen as the first cargo for $P_{55}C_{55}LV$ -mediated cellular delivery. $P_{55}C_{55}LV$ containing PC labeled with NBD or TF in the alkyl chain were administered to the medium of primary human umbilical vein endothelial cells (HUVEC), and the uptake and intracellular fate of the phospholipid were visualized by confocal fluorescence microscopy. Figure 2 shows that 2 h after addition of the NBD-PC carrying $P_{55}C_{55}LV$, the NBD label was distributed throughout the cytosol showing a somewhat reticular pattern with a minor enrichment in the perinuclear region. A similar uptake and distribution pattern, showing increased cytosolic delivery with time, was observed for TF-PC (Figure S8, Supporting Information). The distribution of NBD- or TF-labeled PC after $P_{55}C_{55}LV$ -mediated delivery into HUVEC looked reminiscent of the endoplasmic reticulum (ER)

and co-staining with an ER-marker indeed revealed considerable co-localization (Figure S9, Supporting Information).

We also analyzed the intracellular fate of the $P_{55}C_{55}LV$ polymer shell after delivery into HUVEC. Therefore, an amine-functionalized fluorophore, Dy633, was attached during the crosslinking process by covalent linkage to acrylic acid moieties of the polymer shell. After internalization of this modified $P_{55}C_{55}LV$, the polymer shell label did not distribute throughout the cytoplasm but appeared in punctate structures that were identified as endosomes by simultaneous uptake of rhodamine B (RhB) conjugated dextran (RhB-Dextran, $M_n \approx 70$ kDa) (Figure 2). Together, these results suggest that the $P_{55}C_{55}LV$ are first internalized into the endosomal system before the reductive environment of endosomes triggers disintegration of the redox-sensitive polymer shell and β -CD₅₅ core. The degraded polymer shell remains trapped in endosomes whereas the amphiphilic cargo, i.e., the labeled phospholipids, is released

from the disintegrated $P_{SS}C_{SS}LV$ and escapes from endosomes to partition into ER membranes. The enrichment in the ER probably reflects the ubiquitous nature of ER membranes that comprise the majority of intracellular membranes.

To verify the regulatory role of the two disulfide crosslinks and show that cleavage indeed occurs in endosomes, we

performed control experiments with both nonredox-responsive PCLV and shell-free $C_{SS}LV$. In the case of the shell-free $C_{SS}LV$ -containing NBD-PC, only a very limited amount of aggregated structures residing outside of the cells, but no significant cellular uptake is observed (**Figure 3**). Most likely this is due to inefficient endocytosis and/or compromised stability

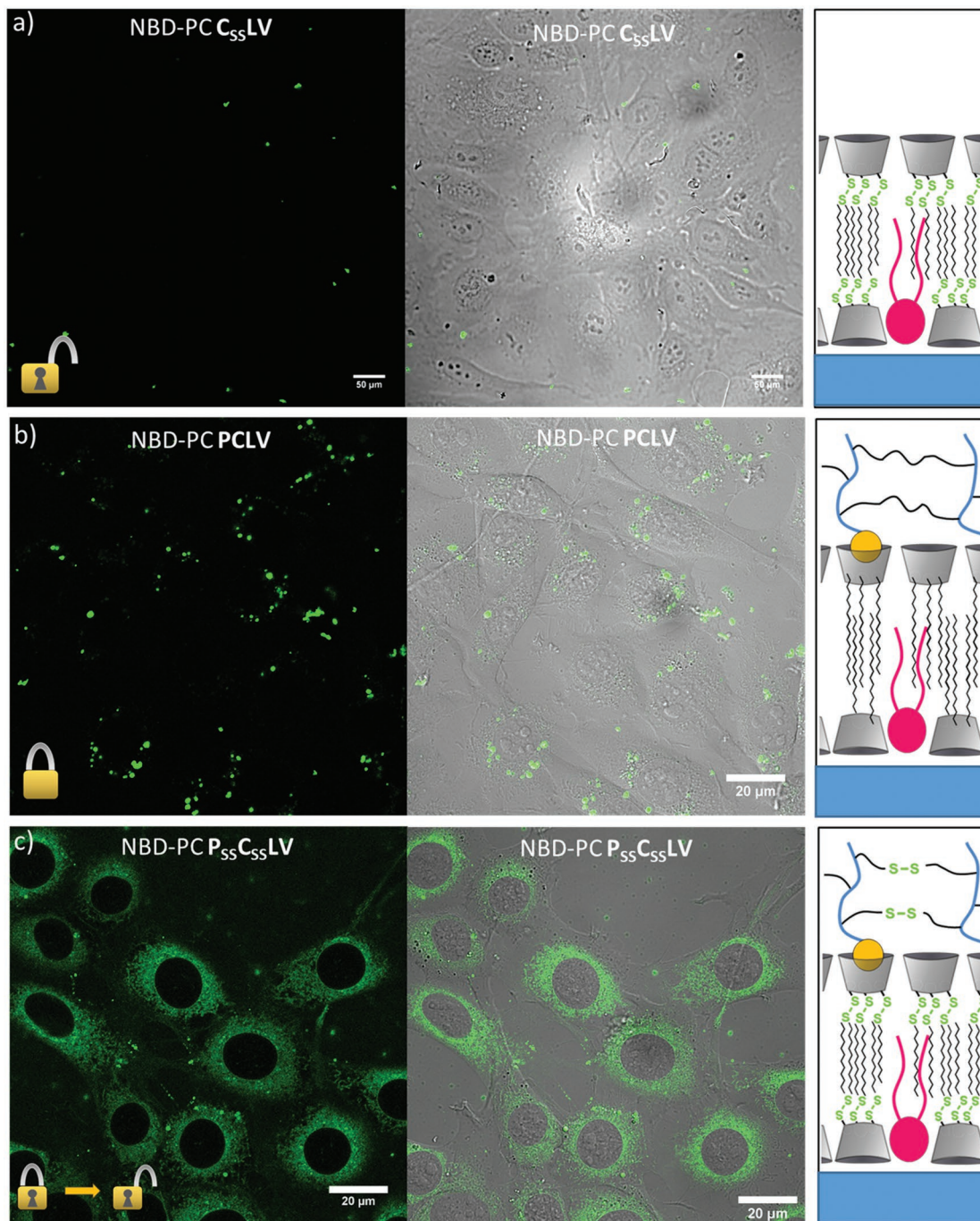


Figure 3. Uptake and endosomal escape of NBD-PC incorporated into different types of nanocontainers. Three different types of containers were analyzed for their capacity to deliver labeled PC into the cytosol of cultivated HUVEC. a) “Open” containers, $C_{SS}LV$, consisting of a redox-sensitive β - CD_{SS} core without a polymer shell. Small aggregates visible on top of the HUVEC layer most likely represent noninternalized containers. b) “Closed” containers, PCLV, containing only nonredox-responsive units. These are taken up into punctuate structures but the labeled PC is not released into the cytosol. c) Redox-sensitive containers, $P_{SS}C_{SS}LV$, with a redox-responsive core and a redox-responsive shell, are internalized and the labeled phospholipids are released into the cytosol.

of the $C_{55}LV$ in the absence of a polymer shell. Nonredox-responsive PCLV harboring NBD-PC, on the other hand, were internalized into endosomes, but the labeled phospholipid remained entrapped and was not transported to ER membranes (Figure 3). Only the fully redox-responsive polymer-shelled $P_{55}C_{55}LV$ containers were efficiently internalized and released their fluorophore-PC cargo into the cytosol. This indicates that the polymer shell significantly increases stability and endocytic uptake and that both; a reductively cleavable polymer shell and β -CD $_{55}$ core are required for efficient release of labeled phospholipids into the cytosol (Figure 3). Thus, $P_{55}C_{55}LV$ represent an alternative cellular uptake and cargo delivery system exploiting redox sensitivity similar to disulfide-based and thus reduction-sensitive polymersomes described recently.^[28–32]

We next examined the cellular delivery of other fluorescently labeled phospholipids incorporated into the redox-responsive $P_{55}C_{55}LV$ containers. NBD-PA-containing $P_{55}C_{55}LV$ were also efficiently internalized into endosomes from where the NBD-PA was released into the cytosol accumulating in structures at least in part representing ER membranes. Control experiments with redox-stable PCLV containers again showed that the cytosolic transport of NBD-PA depended on the presence of a reductively cleavable disulfide bond both, in the β -CD $_{55}$ core and in the polymer shell (Figure S10, Supporting Information).

Phosphoinositides (PI) represent another class of negatively charged phospholipids characterized by a highly hydrophilic headgroup that is subject to phosphorylation at different positions. To also analyze this subgroup of phospholipids, we assessed the $P_{55}C_{55}LV$ -mediated uptake of different PIs. TF-PI-containing $P_{55}C_{55}LV$ were again efficiently internalized into the endosomal structures. However, at 2 h post delivery only a relatively small portion of the labeled PI appeared in the cytosol, whereas a noticeable signal of TF-PI remained associated with RhB-dextran labeled endosomes. Only prolonged incubation times resulted in substantial cytosolic delivery (Figure S11, Supporting Information). Endosomal retention is even more pronounced in case of the dual phosphorylated PI(4,5)P $_2$. When delivered in $P_{55}C_{55}LV$, TF-PI(4,5)P $_2$ remained in RhB-dextran positive endosomes for extended period of time, and even after 24 h no significant release to the cytosol was observed. Since the redox-induced disassembly of the $P_{55}C_{55}LV$ within endosomes is most likely not dependent on the encapsulated amphiphilic cargo, the difference in cytosolic release kinetics between PC and PA on one hand and phosphoinositide derivatives on the other hand is most likely due to the different head groups. Although the mechanism that triggers the release of the $P_{55}C_{55}LV$ delivered phospholipids from endosomes is not known, the different kinetics observed here argue for an important role of the head group, possibly by affecting a translocation from the luminal to the cytoplasmic leaflet of the endosomal bilayer. It should be noted that after release of the fluorescently labeled lipid from the $P_{55}C_{55}LV$ a further biosynthetic modification of the lipid can occur, both, in endosomes and even more likely at the ER. However, the significant head group differences observed here indicate that major processes such as a rapid degradation of the lipid are unlikely to occur.

In conclusion, we synthesized polymer-shelled nanocontainers based on redox-responsive cyclodextrin amphiphiles which were able to deliver different types of fluorescently

labeled phospholipids (PC, PA, and PI) to intracellular membrane compartments (endosomes, ER). Mixtures of reductively degradable cyclodextrin amphiphiles and different phospholipids formed liposome-like cyclodextrin vesicles ($C_{55}LV$) with a homogeneous distribution of each lipid. $C_{55}LV$ could be encapsulated in a redox-sensitive polymer shell, and the resulting $P_{55}C_{55}LV$ showed a high stability that was regulated by the redox state of the environment. $P_{55}C_{55}LV$ were efficiently internalized into endosomes of primary human endothelial cells where the incorporated amphiphilic cargo was released via reductive disintegration of the $P_{55}C_{55}LV$. We also showed that $P_{55}C_{55}LV$ represent a novel tool to deliver fluorescently labeled phospholipids into cells and that the endosomal escape of these externally delivered phospholipids depends on the type of head group. Thus, $P_{55}C_{55}LV$ represent a highly efficient transport system for the delivery of lipid-like amphiphilic cargo into the intracellular environment.

Experimental Section

Methods including DLS, FRET, TEM, and microscopic imaging as well as synthesis of $C_{55}LV$ and $P_{55}C_{55}LV$ are described in detail in the Supporting Information.

Supporting Information

Supporting Information is available from the Wiley Online Library or from the author.

Acknowledgements

W.C.d.V. and S.K. contributed equally to this work. This work was funded by the Deutsche Forschungsgemeinschaft (EXC 1003 Cells in Motion Cluster of Excellence to V.G. and B.J.R.; SFB 858/B19 to A.S., V.G., and B.J.R.; SFB 1348/A04 to V.G.; INST 211/719-1 FUGG for TEM instrumentation).

Conflict of Interest

The authors declare no conflict of interest.

Keywords

disulfides, intracellular delivery, lipids, liposomes, polymers, self-assembly

Received: July 26, 2019
Revised: October 6, 2019
Published online: October 24, 2019

- [1] M. Cebeauer, M. Amaro, P. Jurkiewicz, M. J. Sarmiento, R. Šachl, L. Cwiklik, M. Hof, *Chem. Rev.* **2018**, *118*, 11259.
- [2] E. Muro, G. E. Atilla-Gokcumen, U. S. Eggert, *Mol. Biol. Cell* **2014**, *25*, 1819.
- [3] A. Jain, J. C. M. Holthuis, *Biochim. Biophys. Acta, Mol. Cell Res.* **2017**, *1864*, 1450.

- [4] S. Takatori, R. Mesman, T. Fujimoto, *Biochemistry* **2014**, *53*, 639.
- [5] A. Laguerre, C. Schultz, *Curr. Opin. Cell Biol.* **2018**, *53*, 97.
- [6] A. Csiszar, N. Hersch, S. Dieluweit, R. Biehl, R. Merkel, B. Hoffmann, *Bioconjugate Chem.* **2010**, *21*, 537.
- [7] S. Du, S. S. Liew, L. Li, S. Q. Yao, *J. Am. Chem. Soc.* **2018**, *140*, 15986.
- [8] S. Kube, N. Hersch, E. Naumovska, T. Gensch, J. Hendriks, A. Franzen, L. Landvogt, J. P. Siebrasse, U. Kubitscheck, B. Hoffmann, R. Merkel, A. Csiszar, *Langmuir* **2017**, *33*, 1051.
- [9] J. J. Richardson, J. W. Maina, H. Ejima, M. Hu, J. Guo, M. Y. Choy, S. T. Gunawan, L. Lybaert, C. E. Hagemeyer, B. G. De Geest, F. Caruso, *Adv. Sci.* **2015**, *2*, 1400007.
- [10] X. Zhang, C. Xu, S. Gao, P. Li, Y. Kong, T. Li, Y. Li, F. Xu, J. Du, *Adv. Sci.* **2019**, *6*, 1900386.
- [11] G. Saravanakumar, J. Kim, W. J. Kim, *Adv. Sci.* **2017**, *4*, 1600124.
- [12] A. S. Klymchenko, R. Kreder, *Chem. Biol.* **2014**, *21*, 97.
- [13] M. Stöckl, A. P. Plazzo, T. Korte, A. Herrmann, *J. Biol. Chem.* **2008**, *283*, 30828.
- [14] K. Niikura, K. Nambara, T. Okajima, Y. Matsuo, K. Ijiro, *Langmuir* **2010**, *26*, 9170.
- [15] M. Massignani, I. Canton, T. Sun, V. Hearnden, S. MacNeil, A. Blanazs, S. P. Armes, A. Lewis, G. Battaglia, *PLoS One* **2010**, *5*, e10459.
- [16] L. Chierico, A. S. Joseph, A. L. Lewis, G. Battaglia, *Sci. Rep.* **2015**, *4*, 6056.
- [17] J. Dong, Y. Tang, A. L. Lewis, S. P. Armes, *J. Am. Chem. Soc.* **2006**, *127*, 17982.
- [18] D. Nolan, R. Darcy, B. J. Ravoo, *Langmuir* **2003**, *19*, 4469.
- [19] W. C. de Vries, D. Grill, M. Tesch, A. Ricker, H. Nüsse, J. Klingauf, A. Studer, V. Gerke, B. J. Ravoo, *Angew. Chem., Int. Ed.* **2017**, *56*, 9603.
- [20] S. A. Dergunov, S. C. Schraub, A. Richter, E. Pinkhassik, *Langmuir* **2010**, *26*, 6276.
- [21] S. A. Dergunov, B. Miksa, B. Ganus, E. Lindner, E. Pinkhassik, *Chem. Commun.* **2010**, *46*, 1485.
- [22] M. R. Lee, D. J. Brown, C. L. Smith, M. E. Hodson, M. MacKenzie, R. Hellmann, *Am. Mineral.* **2007**, *92*, 1383.
- [23] L. E. Franken, E. J. Boekema, M. C. A. Stuart, *Adv. Sci.* **2017**, *4*, 1600476.
- [24] B. J. Ravoo, R. Darcy, *Angew. Chem., Int. Ed.* **2000**, *39*, 4324.
- [25] P. Falvey, C. W. Lim, R. Darcy, T. Revermann, U. Karst, M. Giesbers, A. T. M. Marcelis, A. Lazar, A. W. Coleman, D. N. Reinhoudt, B. J. Ravoo, *Chem. - Eur. J.* **2005**, *11*, 1171.
- [26] A. Samanta, M. Tesch, U. Keller, J. Klingauf, A. Studer, B. J. Ravoo, *J. Am. Chem. Soc.* **2015**, *137*, 1967.
- [27] J. E. Vance, *Traffic* **2015**, *16*, 1.
- [28] C. Nehate, A. A. M. Raynold, V. Haridas, V. Koul, *Biomacromolecules* **2018**, *19*, 2549.
- [29] K. Goyal, A. Konar, B. S. H. Kumar, V. Koul, *Nanoscale* **2018**, *10*, 17781.
- [30] R. Bej, J. Sarkar, D. Ray, V. K. Aswal, S. Ghosh, *Macromol. Biosci.* **2018**, *18*, 1800057.
- [31] S. Pottanam Chali, B. J. Ravoo, *Angew. Chem., Int. Ed.* **2019**, <https://doi.org/10.1002/anie.201907484>.
- [32] C. Nehate, A. Nayal, V. Koul, *ACS Biomater. Sci. Eng.* **2019**, *5*, 70.